computation

MDPI

Article

What Is an Oval, Officially and Overall? Old and New Mathematical Descriptions

Valeriy G. Narushin [1], Stefan T. Orszulik [2], Michael N. Romanov [3,4,*] and Darren K. Griffin [3,4]

[1] Independent Researcher, Soborny 145-B, 69035 Zaporizhya, Ukraine; valnarushin@gmail.com
[2] Independent Researcher, Grove, Wantage, Oxfordshire OX12 0QA, UK; s.orszulik@ntlworld.com
[3] School of Natural Sciences, University of Kent, Canterbury, Kent CT2 7NJ, UK; d.k.griffin@kent.ac.uk
[4] Animal Genomics and Bioresource Research Unit (AGB Research Unit), Faculty of Science, Kasetsart University, Chatuchak, Bangkok 10900, Thailand
* Correspondence: m.romanov@kent.ac.uk

Abstract

Deriving from the Latin "ovum" (egg), the oval is a commonly used term, but does not have the status of a standard geometric figure like a circle or ellipse. Consequently, the oval lacks both a mathematical descriptive basis to attribute a set of key geometric parameters and an elegant formula to describe its contours. Herein, we consider the basis for deriving the formula of an oval for typical egg profiles. Specifically, these are round, ellipsoid, classic oval, pyriform (conical) and biconical shapes. To do this, we adhered to four basic postulates: (i) the ability to describe all possible egg shapes; (ii) a minimum set of measurable geometric parameters; (iii) the application of some universal indices (ratios of key geometric dimensions) to describe mathematical models; (iv) conformity with the "Main Axiom of the Mathematical Formula of the Bird's Egg." Additionally, we sought to comply with the principles of mathematical elegance. Following these theoretical assumptions and practical verification, we obtained a mathematically supported, elegant formula for this well-known but non-standardized geometric figure. The derived oval geometry equation will find use in applied problems of biology, construction, engineering and school curricula, alongside the classical figures of the circle and ellipse.

Keywords: oval; egg shapes; egg geometry; pyriform eggs; biconical eggs; reptilian eggs; superellipse; Hügelschäffer's model; Narushin's model

> *"God Always Plays the Geometer".*
> Plutarch, *Moralia*, *Quaestiones Convivales* [1,2].

1. Introduction

The range of standard geometric shapes has its basis in the time of Plato and other ancient thinkers [1,2]. Moreover, the diversity of egg shapes is a mainstay study of ornithologists, evolutionists and aviculturists, and serves as a source of inspiration for works of art [3–7], architectural structures [8–11], and design objects [7,12]. An "egg-like" geometric structure is typically called an 'oval', the name of which derives from the Latin *ovum* [13]. Despite the regular use of the term oval, however, it is most often used as a qualitative, rather than quantitative description of an object (including ellipses), with a wide range of geometric characteristics [14]. It is also thought to have a set of other specialized curves that conditionally resemble an egg, for example, Cartesian (e.g., [15]) or Cassini ovals (e.g., [16]). Dixon [17] laid out the principles of the geometric construction of ovals, representing them as *"a smooth curve by joining several circular arcs of different radii."* He proposed basing ovals

Academic Editor: Rainer Breitling

Received: 24 March 2026
Revised: 19 April 2026
Accepted: 24 April 2026
Published: 27 April 2026

on the four basic varieties inherent in real eggs found in nature, which are commonly referred to as round, ellipsoid, classic oval, and conical (pyriform, or pear-shaped). To visualize these shapes, we used images of corresponding bird eggs (Figure 1).

(**a**) (**b**) (**c**) (**d**)

Figure 1. Examples of egg profiles: (**a**) spherical, of the pied kingfisher (*Ceryle rudis*) [18]; (**b**) ellipsoid, of the blue-spotted wood dove (*Turtur afer*) [19]; (**c**) classic oval, of the harlequin duck (*Histrionicus histrionicus*) [20]; (**d**) conic, or pyriform, of the common redshank (*Tringa totanus*) [21].

Since it is extremely difficult to find a perfect match, with standard geometric shapes, there is a tendency to consider similarity, i.e., the maximum approximation of actual eggs to their theoretical counterparts.

There is a wide range of intermediate egg shapes in nature that fall between the principle geometric oval construction established by Dixon [17]. For example, Biggins et al. [22] expanded the range of their varieties to 10, while Mytiai and Matsyura [23] and Mytiai et al. [24] expanded it to 80. Nevertheless, the four classical forms of bird eggs remain the most common types used in applying mathematical interpretations (e.g., [25–27]). This relative simplicity of categorization is, however, increased by eggs of the so-called biconical profile, sometimes distinguished by researchers as a separate geometric form (e.g., [28,29]). The biconical profile is characterized by a slight sharpening at the blunt end (Figure 2).

(**a**) (**b**) (**c**)

Figure 2. Examples of biconical eggs: (**a**) isabelline wheatear (*Oenanthe isabellina*) [30]; (**b**) rook (*Corvus frugilegus*) [31]; (**c**) red-necked grebe (*Podiceps grisegena*) [32].

The difficulty in describing the biconical shape lies in the fact that the initial shape for the mathematical model is either an ellipse, as in the Hügelschäffer's [26,27,33] and Smart's [34] models, or a circle, as in the Preston model [35,36]. Moreover, only one end of the oval undergoes a mathematical transformation, making it sharper, thus introducing an

additional function into the calculation. The shape of the blunt end remains unchanged. It is possible that the similarity of an egg to an ellipse is a certain perceptual barrier in the search for the optimal basis for the oval model, indirectly preventing the authors from going beyond the established analogy.

To take its place as a recognized geometric shape among such popular figures as a circle or an ellipse, the oval requires both a mathematical descriptive basis, which could include a set of key geometric parameters, and an elegant formula for reproducing its contours. Such attempts have already been made, not for the purposes of classical geometry, but as applied problems related to research in the fields of commercial poultry production [37–39] or oology, as a subdivision of ornithology [34,35,40].

Our previous works described eggs in nature according to fundamental geometric laws [26,27]. We paid close attention to the issue of mathematical standardization of bird egg contours, which can be fully adopted as a basis for a broader geometric group of ovals. In our review paper [41] on using mathematical models to evaluate various parameters and characteristics of bird eggs, we formulated several basic principles, these being:

1. The ability to describe all possible types of egg shapes, i.e., from classic ovals to pear-shaped contours [26].
2. The minimum acceptable set of measurable geometric parameters of an oval and, as such, there can be no more than four according to our research [26,27]. These are its length (L), maximum breadth (B), the distance (w) by which the maximum breadth of the oval is shifted from its center, i.e., from the point $x = L/2$, and the diameter (D_p) of the oval at a point $L/4$ from its pointed end. For ease of visual perception, these parameters are depicted in Figure 3.

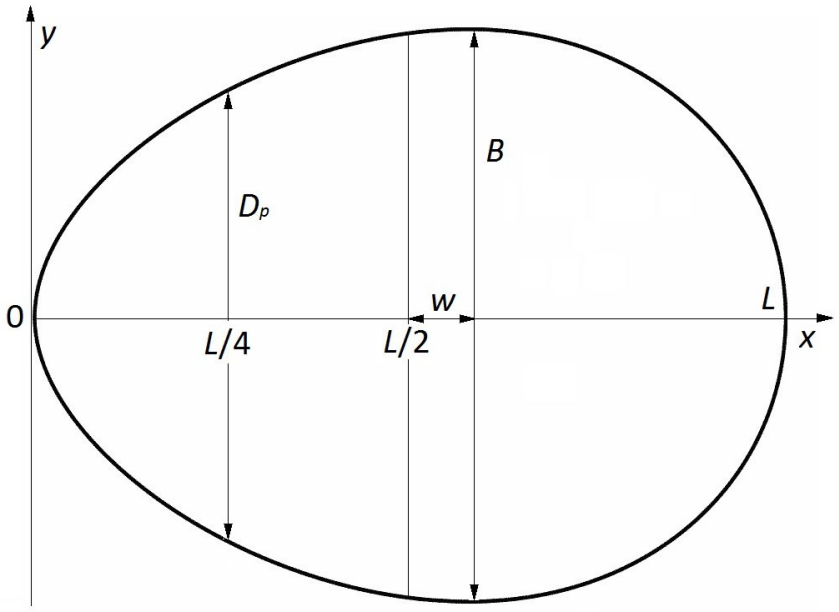

Figure 3. Schematic representation of a set of key geometric parameters of an ovoid.

3. The possibility of representing the model in the form of universal indices reflecting the ratios of key geometric dimensions. According to our research [26,27,41–43], the following can be adopted as basic ones: the shape index (B/L), the asymmetry index (w/L), and the conicity index (D_p/B).
4. As a fundamental condition for the oval's mathematical formula to comply with the classical law of geometry, we postulated the "Main Axiom of the Mathematical Formula of the Bird's Egg," hereafter the "Main Axiom" [27]. This axiom basically states that the value of $B/2$, or half the maximum diameter of the egg, should be the

extremum of the function that characterizes the geometry of the egg contour. Failure to comply with the principles of the Main Axiom essentially means non-conformity of the exact position of the maximum breadth. Therefore, this approach may become the basis for assessing the adequacy of and compliance with the principles of universality and standardization of the oval's mathematical formula. The theoretical implication of the Main Axiom is the interior extremum theorem, also known as Fermat's theorem, according to which, at the local extrema of a differentiable function, its derivative is always zero (e.g., [44]). Accordingly, for a differentiable function, the vanishing of the derivative is a necessary condition for the existence of a local extremum. Consequently, if a model predicts the absence of a zero derivative at a point where, for geometric reasons, the extremum should be located, such a model inadequately describes the studied object.

As an additional requirement, we would propose the condition that it would be highly advisable for the oval formula to comply with the principles of "mathematical elegance". The concept of mathematical elegance can be roughly expressed by the following phrase: "Minimality with maximum meaning." That is, an elegant formula expresses a lot of content with little means, i.e., a minimum of symbols. It has the absence of so-called "technical garbage" (unnecessary coefficients, indices, exceptions) and the presence of only functionally necessary elements (e.g., [45,46]). Common equations of such geometric figures as a circle and an ellipse are clear examples of mathematical elegance. However, each of them can be described by much more complex formulae, e.g., higher-order polynomials (e.g., [47,48]).

Judging from the above requirements, we began work on evaluating and potentially improving well-known egg contour models that are popular among researchers working in this field. In particular, this concerned the most popular mathematical formulae, such as Hügelschäffer's model [27,33], Preston's model [49], Smart's model [50], and Baker's model [51]. None of these mathematical relationships could, however, claim full compliance with the proposed criteria. For example, the Preston, Smart and Baker models do not demonstrate compliance with the Main Axiom. Moreover, attempts at implementing mathematical transformations to ensure compliance led to inaccuracies in contour reproduction [50,51]. The Preston model, as interpreted by Biggins et al. [36], demonstrated a fairly accurate reproduction of egg contours; however, this required measurements of five initial parameters that were different from those proposed as basic in Figure 3 [49], which, moreover, cannot be represented in the form of three recommended indices (shape, asymmetry, and conicity).

Hügelschäffer's model [27] was the most suitable in terms of its compliance with the four fundamental principles of deriving the oval equation. However, its mathematical form is far from elegant. The formula is clearly artificial, as it represents a mathematical description of two egg halves (pointed and blunt), "sewn" together by an additional connecting equation used to combine piecewise functions.

When it comes to mathematical elegance, one cannot overlook the attempts to represent egg contours using polar coordinates. This presentation appears quite succinct. However, its elegance is lost when transformed into a Cartesian form. For example, the rather simple and elegant formula of Narushin's model [39] expressed in polar coordinates:

$$r = L \cdot \cos^n \theta, \quad (1)$$

in which r is the polar radius, θ is the polar angle, L is the maximum length of the egg, and n is a rational non-negative number. The equation acquires a somewhat more complicated equation when transformed into a Cartesian form:

$$y = \pm\sqrt{L^{\frac{2}{n+1}} x^{\frac{2n}{n+1}} - x^2}. \quad (2)$$

When using the so-called superformula [52] to describe the contours of eggs [53], the authors, despite using a simplified version of this mathematical expression, limited themselves to its polar notation without attempting to transform it into Cartesian coordinates:

$$r(\varphi) = a\left(|\cos(\varphi/4)|^{n_2} + |\sin(\varphi/4)|^{n_2}\right)^{-1/n_1}, \quad (3)$$

where r is the polar radius at the polar angle φ, and a, n_1, and n_2 are parameters to be estimated.

The transformation of the polar equation (3) into the more convenient system $y = f(x)$ is complicated by the presence of the fractional angle function $(\varphi/4)$. A similar situation is observed in the polar formula of Carter and Jones [54], with the only difference being that the authors used double angle functions:

$$r = K_1 + K_2 \cos 2\theta + K_3(-\cos^3\theta) + K_4(-\sin^2 2\theta) + K_5 \sin^3 2\theta, \quad (4)$$

where $K_1 \ldots K_5$ is a set of coefficients, the values of which are determined depending on the shape of the actual egg.

Polar coordinates are well-suited for compact formulae, but poorly suited for rigorous morphometry. According to Wang et al. [55], *"this may be attributed to their complex model structure and the lack of explicit geometric interpretations for the equation parameters."* That is, in an egg model defined in polar coordinates, only the length is most often specified. The breadth is a derived parameter, which can lead to geometric inaccuracies. Consequently, model parameters often lack a clear geometric meaning, and the coefficients used cannot be directly compared between different objects.

Here, we consider exploiting the positive qualities, particularly the simplicity and elegance, of the polar representation of ovals using the trigonometric functions inherent in this form of mathematical expression. Indeed, sine and/or cosine waves have a significant property, i.e., the constant coordinate of the extremum point. This is precisely the essence of the Main Axiom. Thus, the purpose of this study was to develop a mathematical formula for ovals that would conform to any variety of eggs, including, in addition to the classic ones, such exotics as pear-shaped and biconical (Figures 1 and 2). It is our intention that this would (a) meet the stated requirements, including the criterion of elegance, and (b) use a trigonometric function as the basic equation.

2. Theory

We first adopted our own published (Narushin's) model [39], which, in addition to its mathematical simplicity, has found popularity in industrial poultry farming [56–60] and in the engineering industry [61–67]. The only change, besides replacing the variables r with y and x, was the use of the 'sin' function instead of 'cos' (Equation (1)). This was explained by the fact that sine and cosine graphs are identical wave shapes but are phase-shifted by $\pi/2$ radians, i.e., if the sine graph starts at the origin (0, 0) and rises, while the cosine graph starts at its peak (0, 1) and falls (e.g., [68]). Since the preferred location of the oval for our

case is in the interval (0, L) (Figure 3), using the sine function is clearly preferable. Based on this logical reasoning, the basic equation of the oval was written as follows:

$$y = \pm a \sin^n x. \tag{5}$$

It turns out that such an equation has already been considered by Köller [69] for $n = 0.5$. Indeed, the resultant image resembles an egg outline.

The coefficient a in Equation (5) does not correspond to the length of the oval (L), as in Equation (1), but is nothing more than the amplitude of the sinusoid (e.g., [70]) that, in our case, is equal to half the maximum breadth of the oval ($B/2$). Then, Equation (5) can be rewritten as follows:

$$y = \pm \frac{B}{2} \sin^n x. \tag{6}$$

A serious limitation of the Narushin model (Equation (1)) is that the value of the exponent n depends only on the shape index, i.e., B/L [39,66]. However, in accordance with the proposed conditions for the adequacy of the oval equation, two more indices should be considered, i.e., w/L and D_p/B. Therefore, two additional coefficients should be introduced into Equation (6); let us call them b and c. Then, with three coefficients (n, b, and c), it will be possible to evaluate fully possible variations in the oval shape using all three (shape, asymmetry and conicity) indices. The most convenient option for providing additional coefficients is some restructuring of the argument. That is, instead of a single variable x in Equation (6), a sub-function should be added that should meet a set of conditions. First, it should contain the two missing coefficients (b and c); and second, it should satisfy the condition that at the initial coordinate point, that is, when $x = 0$, y should also be equal to 0. After trying out possible options, we settled on the following sub-functions:

- Incomplete polynomial (without constant term) of degree 2: $bx^2 + cx$.
- Power function: bx^c.
- Rational function: $\frac{bx}{x+c}$.
- Product of variable x and exponential function: $bx \cdot c^x$.
- Exponential combination: $b(c^x - 1)$.

Thus, we have at our disposal five functions based on a sinusoid and one of the listed sub-functions included in it:

$$y = \pm \frac{B}{2} \sin^n \left(bx^2 + cx \right), \tag{7}$$

$$y = \pm \frac{B}{2} \sin^n (bx^c), \tag{8}$$

$$y = \pm \frac{B}{2} \sin^n \left(\frac{bx}{x+c} \right), \tag{9}$$

$$y = \pm \frac{B}{2} \sin^n (bx \cdot c^x), \tag{10}$$

$$y = \pm \frac{B}{2} \sin^n (b(c^x - 1)). \tag{11}$$

Next, we derived equations for determining the coefficients n, b and c, for which the following governing conditions were specified based on the geometric dimensions presented in Figure 3:

1. When $y = 0$, $x = 0$ or L. Given that the value $x = 0$ does not allow us to derive an adequate mathematical relationship, we chose the option $x = L$.
2. When $y = D_p/2$, $x = L/4$.
3. When $y = B/2$, $x = L/2 + w$.

The above conditions are sufficient to derive equations for n, b, and c and/or mathematically transform the corresponding Formulae (7)–(11) into their final form. A detailed description of the calculations for each formula is presented in the Supplementary Data.

It is often much more convenient to operate with a unit oval length (equal to 1), determined graphically in the interval [0...1]. For this purpose, in addition to the classical form of representing dependencies (7)–(11) as $y = f(x)$, we used their transformation as functions $y/L = f(x/L)$. The obtained results of five types of mathematical models (Equations (7)–(11)), which we will conventionally name in accordance with the name of their sine sub-functions, along with the calculation formulae for defining the exponent n, took the following form:

I. Incomplete polynomial:

$$y = \pm\frac{B}{2}\sin^n\left\{\frac{\pi}{\frac{1}{4}-\left(\frac{w}{L}\right)^2}\left(\frac{w}{L}\left(\frac{x}{L}\right)^2+\left[\frac{1}{4}-\frac{w}{L}-\left(\frac{w}{L}\right)^2\right]\frac{x}{L}\right)\right\}, \tag{12}$$

$$\frac{y}{L} = \pm\frac{1}{2}\cdot\frac{B}{L}\sin^n\left\{\frac{\pi}{\frac{1}{4}-\left(\frac{w}{L}\right)^2}\left(\frac{w}{L}\left(\frac{x}{L}\right)^2+\left[\frac{1}{4}-\frac{w}{L}-\left(\frac{w}{L}\right)^2\right]\frac{x}{L}\right)\right\}, \tag{13}$$

in which

$$n = \frac{\ln\left(\frac{D_p}{B}\right)}{\ln\left(\sin\left[\frac{\pi}{4}\cdot\frac{1-3\frac{w}{L}-4\left(\frac{w}{L}\right)^2}{1-4\left(\frac{w}{L}\right)^2}\right]\right)}. \tag{14}$$

II. Power function:

$$y = \pm\frac{B}{2}\sin^n\left[\frac{\pi}{\left(\frac{x}{L}\right)^{\frac{0.69315}{\ln\left(\frac{1}{2}+\frac{w}{L}\right)}}}\right], \tag{15}$$

$$\frac{y}{L} = \pm\frac{1}{2}\cdot\frac{B}{L}\sin^n\left[\frac{\pi}{\left(\frac{x}{L}\right)^{\frac{0.69315}{\ln\left(\frac{1}{2}+\frac{w}{L}\right)}}}\right], \tag{16}$$

in which

$$n = \frac{\ln\left(\frac{D_p}{B}\right)}{\ln\left[\sin\left(\pi\cdot 2.614^{\frac{1}{\ln\left(\frac{1}{2}+\frac{w}{L}\right)}}\right)\right]}. \tag{17}$$

III. Rational function:

$$y = \pm\frac{B}{2}\sin^n\left(\pi\frac{\left(\frac{w}{L}-\frac{1}{2}\right)\frac{x}{L}}{\frac{w}{L}\left(2\frac{x}{L}-1\right)-\frac{1}{2}}\right), \tag{18}$$

$$\frac{y}{L} = \pm\frac{1}{2}\cdot\frac{B}{L}\sin^n\left(\pi\frac{\left(\frac{w}{L}-\frac{1}{2}\right)\frac{x}{L}}{\frac{w}{L}\left(2\frac{x}{L}-1\right)-\frac{1}{2}}\right), \tag{19}$$

in which

$$n = \frac{\ln\left(\frac{D_p}{B}\right)}{\ln\left[\sin\left(\frac{\pi}{2}\cdot\frac{\frac{1}{2}-\frac{w}{L}}{1+\frac{w}{L}}\right)\right]}. \tag{20}$$

IV. The product of x and the exponential function:

$$y = \pm\frac{B}{2}\sin^n\left[\pi\frac{x}{L}\left(1+2\frac{w}{L}\right)^{\frac{\frac{x}{L}-1}{\frac{1}{2}-\frac{w}{L}}}\right], \tag{21}$$

$$\frac{y}{L} = \pm\frac{1}{2}\cdot\frac{B}{L}\sin^n\left[\pi\frac{x}{L}\left(1+2\frac{w}{L}\right)^{\frac{\frac{x}{L}-1}{\frac{1}{2}-\frac{w}{L}}}\right], \tag{22}$$

in which

$$n = \frac{\ln\left(\frac{D_p}{B}\right)}{\ln\left\{\sin\left[\frac{\pi}{4\left(1+2\frac{w}{L}\right)^{\frac{3}{4\left(\frac{1}{2}-\frac{w}{L}\right)}}}\right]\right\}}. \tag{23}$$

V. Exponential combination:

$$y = \pm\frac{B}{2}\sin^n\left(\pi\frac{e^{8.4\frac{w}{L}\cdot\frac{x}{L}}-1}{e^{8.4\frac{w}{L}}-1}\right), \tag{24}$$

$$\frac{y}{L} = \pm\frac{1}{2}\cdot\frac{B}{L}\sin^n\left(\pi\frac{e^{8.4\frac{w}{L}\cdot\frac{x}{L}}-1}{e^{8.4\frac{w}{L}}-1}\right), \tag{25}$$

in which

$$n = \frac{\ln\left(\frac{D_p}{B}\right)}{\ln\left[\sin\left(\pi\frac{e^{2.1\frac{w}{L}}-1}{e^{8.4\frac{w}{L}}-1}\right)\right]}. \tag{26}$$

To select a single, optimal formula from the variants I–V, we performed a graphical interpretation to assess their correspondence to actual egg contours. The variability of the generated contours was assessed by substituting different values for the B/L, w/L and D_p/B indices. To capture shape variations, the B/L and D_p/B values were left constant, changing only the w/L values. The results obtained for all five variants are presented in Figure 4.

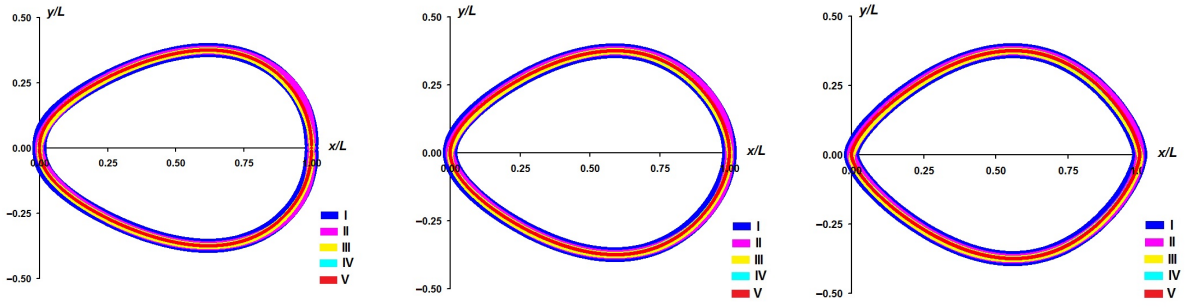

$B/L = 0.75$
$w/L = 0.12$
$D_p/B = 0.72$
(**a**)

$B/L = 0.75$
$w/L = 0.09$
$D_p/B = 0.72$
(**b**)

$B/L = 0.75$
$w/L = 0.06$
$D_p/B = 0.72$
(**c**)

Figure 4. Five variants of oval shape with constant values of B/L (0.75) and D_p/B and gradual change of w/L equal to 0.12 (**a**), 0.09 (**b**) and 0.06 (**c**).

An analysis of the variation in the ovals constructed using five variants of their mathematical interpretation demonstrated an accurate correspondence with one another (Figure 4). Visually, it is difficult to discern clear differences between these variants, although a comparison of the calculated ordinates, as well as a closer examination of each

contour, suggests that such differences exist. The most positive finding is that, using each of the models (variants I–V), we achieved a biconical effect, i.e., the ability to obtain a sharpened blunt end with certain input values (Figure 4c).

Similarly, all five sinusoidal variants can be accurately transformed into the classical geometric figures of a circle and an ellipse. When substituting the index values $B/L = 1$, $w/L = 0$ and $D_p/B = 0.866$ into any of the formulae (Equations (12)–(26)), all sinusoids displayed a perfect circle. The index value $D_p/B = 0.866$ was obtained from the following calculations: using the classical formula for a circle (e.g., [71]):

$$y^2 + x^2 = r^2, \tag{27}$$

in which r is the radius of the circle.

We took into account that its radius is equal to $L/2$. Then, Equation (27) can be rewritten as:

$$y = \sqrt{\frac{L^2}{4} - x^2}. \tag{28}$$

In the resultant Equation (28), we made the respective substitution: $y = D_p/2$, $x = L/4$. Considering that for a circle $L = B$, we have:

$$\frac{D_p}{B} = \frac{\sqrt{3}}{2} \approx 0.866. \tag{29}$$

Similarly, all variants (I–V) demonstrated their conformity to classical ellipses. For the classical ellipse formula (e.g., [72]), we used half the long axis as $L/2$, and, correspondingly, the short axis as $B/2$:

$$y = \frac{B}{L}\sqrt{\frac{L^2}{4} - x^2}. \tag{30}$$

By making the appropriate substitution in Equation (30), i.e., $y = D_p/2$, $x = L/4$, we obtain the same result as for the circle (Equation (29)), that is, $D_p/B \approx 0.866$. However, using sinusoids has a clear advantage over the classical ellipse. This advantage lies in the fact that the value of D_p/B can be reduced or increased, thereby obtaining other types of ovals, from biconical to superellipses, or Lamé curves (e.g., [73,74]). A visualization of the resultant shapes, including a circle and elliptical variations, is presented in Figure 5.

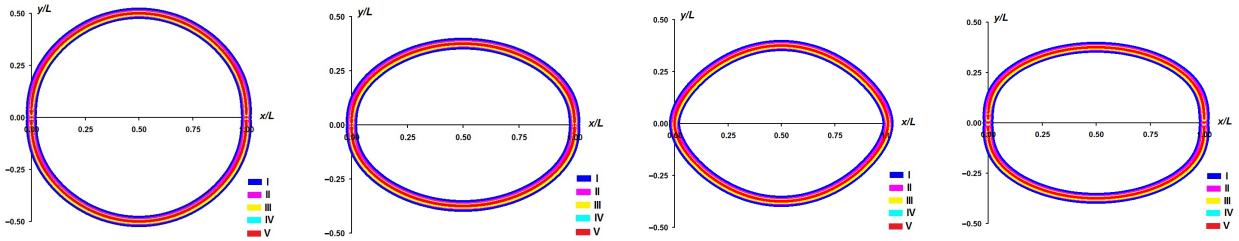

$B/L = 1$
$w/L = 0$
$D_p/B = 0.866$
(**a**)

$B/L = 0.75$
$w/L = 0$
$D_p/B = 0.866$
(**b**)

$B/L = 0.75$
$w/L = 0$
$D_p/B = 0.825$
(**c**)

$B/L = 0.75$
$w/L = 0$
$D_p/B = 0.885$
(**d**)

Figure 5. Five variants of the oval shape transformed into a circle (**a**), a classical ellipse (**b**), a biconical ellipse (**c**), and a superellipse (**d**).

Variations in the classical ellipse (Figure 5c,d) are highly relevant because they significantly expand the possible applications of mathematical equations for ovals. Mytiai and Matsyura [23] classify eggs of this shape as pseudo-ovoid, including representatives of 54 bird families [24]. It is important to note that, in nature, in addition to bird eggs, there are

other egg-laying species. Some of them have a distinct, so-called "cigar-shaped" form. This unusual shape has prompted researchers to develop specific mathematical approaches for the mathematical description of reptile eggs (e.g., [75]). Eggs of a similar shape are also found in the "mysterious" kiwi bird (*Apteryx*). Images of "cigar-shaped" eggs are shown in Figure 6.

(**a**) (**b**)

Figure 6. Examples of cigar-shaped eggs: (**a**) Western pond turtle (*Actinemys marmorata*) [76]; (**b**) common kiwi (*Apteryx australis*) [77].

The possible application of the mathematical equation of the oval, namely in the form of a superellipse, may extend beyond eggs, for example, to describe the contours of different parts of plants (e.g., [78–80]). Geometrically, all the contours shown in Figures 4 and 5 are oval. However, given the need for a mathematical description of the oval, our goal was to settle on a single, optimal model whose shape most closely matches the contours of actual eggs. It is intended that such a mathematical formula could be adopted as the standard for the oval geometric shape. Thus, further experiments had the objective of comparing each of the mathematical models of the variants I–V (Equations (12)–(26)) with various the contours of a range of actual eggs.

3. Materials and Methods

To test the degree of correspondence between each of the mathematical models of the variants I–V (Equations (12)–(26)) and the contours of eggs, we used: (i) a database of digitized images of bird eggs from the Natural History Museum of Wiesbaden, Wiesbaden, Germany [81] and the Muséum de Toulouse [82], which we mathematically processed and used in our previous studies [27,42]; and (ii) geometric profiles of chicken eggs obtained as a result of 2D image scanning [33].

As a result, we had available: (i) the geometric parameters of 444 eggs belonging to 444 avian species, 89 families and 30 orders, representing approximately 4%, 36% and 73% of the entire biodiversity of species, families and orders worldwide; and (ii) 2D scanned images of 40 hen's eggs. These images covered all possible shape variants, which was confirmed by the following index variations: $B/L = 0.55 \ldots 0.95$, $w/L = 0 \ldots 0.15$, and $D_p/B = 0.62 \ldots 0.87$.

For each egg, its geometric shape was generated using Equations (12)–(26) (encompassing the five oval model variants) and compared with the actual digital profile. The correspondence between each theoretical egg profile and the observed outline was quantified using the mean percentage error, ε (e.g., [83]):

$$\varepsilon = \frac{1}{k} \cdot \sum_{1}^{n} \left| \frac{v_1 - v_2}{v_1} \right| \cdot 100\%, \quad (31)$$

where k is the number of x points on the horizontal axis, and v_1 and v_2 are the relevant values of y produced respectively by (1) the direct measurement of the egg profile and (2) computation with the corresponding modification of the mathematical model (Equations (12)–(26)).

Since the goal of our research was to select the oval model that would ensure the most accurate duplication of the egg profile, rather than its absolute copying, taking into account the slightest nuances of shape, we limited ourselves to data on ε. For example, a metric such as the Hausdorff distance [84], developed for image comparison, measures the worst case rather than the typical behavior of contours. That is, the Hausdorff distance reflects extreme deviations rather than overall agreement between shapes. For example, pixel noise, segmentation errors, or microdefects lead to a sharp increase in the Hausdorff distance, although, at the same time, the shape as a whole may match very closely [85]. As a result, biologically irrelevant local irregularities may dominate the Hausdorff distance.

We also considered another common metric, Root Mean Square Error (RMSE), for its suitability in our study. However, RMSE often overestimates large errors, e.g., in cases where outliers dominate, and the mean error is skewed. Also, RMSE assumes normality, which is often not the case in biology. Moreover, RMSE is difficult to interpret because it is presented as a numerical value rather than a percentage discrepancy (e.g., [86–88]).

4. Results and Discussion

A comparison of the results between actual egg profiles and their theoretically generated analogs demonstrated an accurate correspondence for all sub-function variants (I–V). However, considering the combined information for all groups (I–V), the sinusoid with a rational sub-function, i.e., variant III (Equations (18)–(20)), seemed to be superior, albeit by a minimal margin. The results of the comparative investigations for the studied groups of egg shapes are presented below.

4.1. Chicken Eggs as Representatives of Classic Ovals

Previously, while investigating the classical Hügelschäffer's formula [89–92], we [26,33] demonstrated that this model, which may be regarded as a standard of the classical oval shape, is ideally suited for describing chicken eggs. Thus, it can be logically concluded that, when discussing classical oval contours, the shape of a chicken egg can be taken as a basis. As a result of a comparison of actual chicken eggs and theoretically generated oval profiles (Equations (12)–(26)), the following values of ε were obtained:

I. Incomplete polynomial (Equations (12)–(14)), ε = 2.14%.
II. Power function (Equations (15)–(17)), ε = 2.38%.
III. Rational function (Equations (18)–(20)), ε = 2.09%.
IV. The product of x and the exponential function (Equations (21)–(23)), ε = 2.12%.
V. Exponential combination (Equations (24)–(26)), ε = 2.23%.

A visualization of the contours of actual chicken eggs and a sine wave containing a rational sub-function (Equation (19)) is presented in Figure 7. Hereafter, when visualizing the similarity and/or coincidence of the contours of actual eggs with the profile of the generated oval, we decided not to superimpose one image on another, but to place them separately, side by side, so that the smallest nuances of each section of the curves could be more clearly assessed.

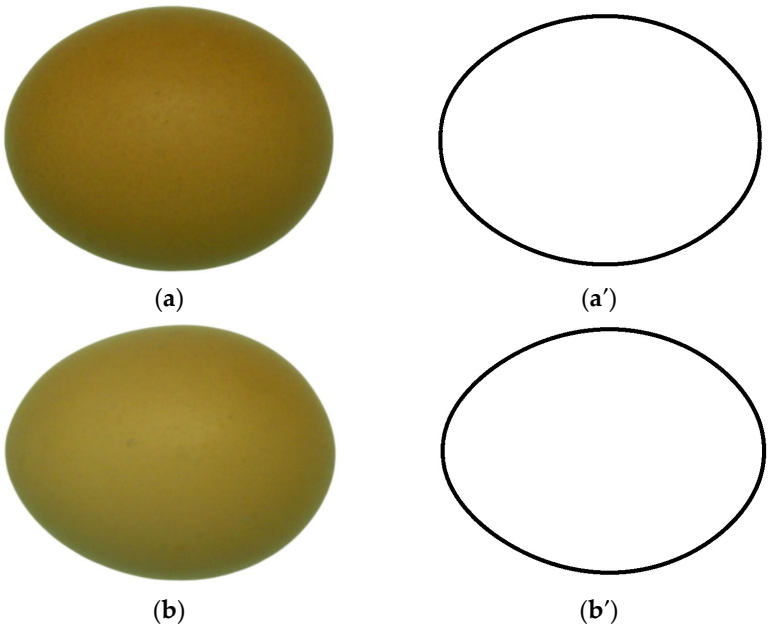

Figure 7. Chicken eggs (**a**,**b**) in comparison to the 'rational' sine function (Equation (19)) (**a′**,**b′**). Eggs (**a**,**b**) were acquired from Woodlands Farm, Canterbury and Staveleys Eggs Ltd., Coppull, UK.

4.2. The Sine Function and Pyriformity

To analyze the ability of the sinusoid to reproduce accurately the contours of pyriform (i.e., pear-shaped, or conical) eggs, we selected 23 eggs from the Natural History Museum of Wiesbaden, Wiesbaden, Germany [81] and the Muséum de Toulouse [82], whose digital profiles we used in our previous studies [27,93]. As a result of a comparison of actual eggs and theoretically generated pear-shaped profiles (Equations (12)–(26)), the following values of ε were obtained:

I. Incomplete polynomial (Equations (12)–(14)), ε = 2.54%.
II. Power function (Equations (15)–(17)), ε = 4.01%.
III. Rational function (Equations (18)–(20)), ε = 2.09%.
IV. The product of x and the exponential function (Equations (21)–(23)), ε = 2.17%.
V. Exponential combination (Equations (24)–(26)), ε = 2.25%.

The visualization comparing the contours of actual pear-shaped eggs and a sinusoid containing a rational sub-function (Equation (19)) is presented in Figure 8.

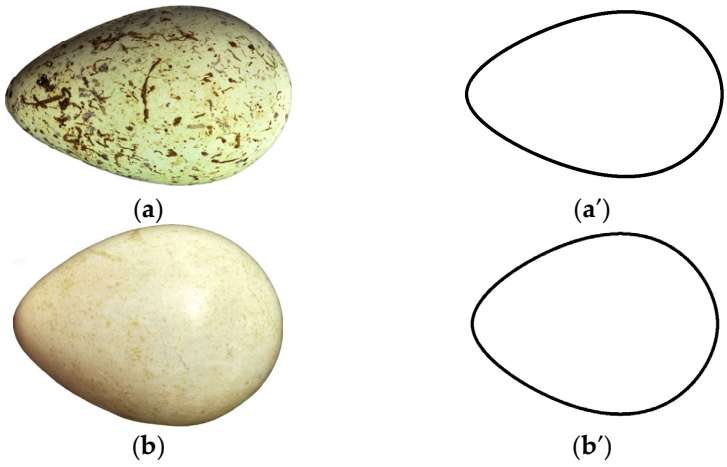

Figure 8. Pyriform eggs (**a**,**b**) in comparison to the 'rational' sine function (Equation (19)) (**a′**,**b′**): (**a**) thick-billed murre (Brünnich's guillemot) (*Uria lomvia*) [94]; (**b**) chukar partridge (*Alectoris chukar*) [95].

4.3. Biconical Eggs

We were able to select only 11 eggs that fit the 'biconical' category. For this group, the power function (Equations (15)–(17)) demonstrated the highest conformity to this shape. Although the differences between variants were small, the power function nevertheless ranked last in this case. A comparative analysis of actual eggs and theoretically generated biconical profiles (Equations (12)–(26)) yielded the following ε values:

I. Incomplete polynomial (Equations (12)–(14)), ε = 2.05%.
II. Power function (Equations (15)–(17)), ε = 1.64%.
III. Rational function (Equations (18)–(20)), ε = 2.14%.
IV. The product of x and the exponential function (Equations (21)–(23)), ε = 2.10%.
V. Exponential combination (Equations (24)–(26)), ε = 1.93%.

To demonstrate the minimal differences for biconical egg profiles using the power (most accurate) and rational (least accurate for this category of eggs) functions, we visualized the matches of the contours of actual eggs and a sinusoid containing the power (Equation (16)) and rational (Equation (19)) sub-functions (Figure 9).

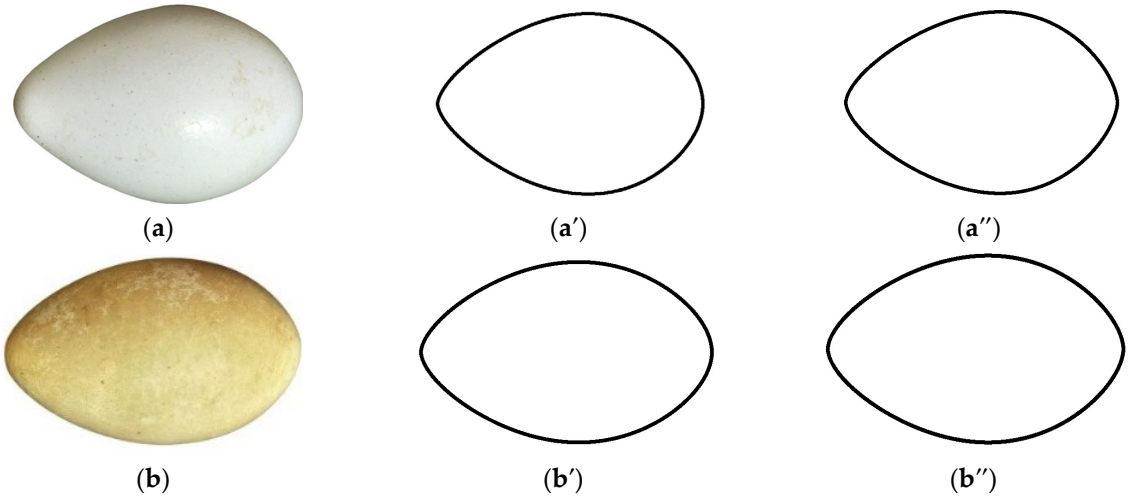

Figure 9. Biconical eggs (**a**,**b**) in comparison to the 'power' sine function (Equation (16)) (**a′**,**b′**) and 'rational' sine function (Equation (19)) (**a″**,**b″**): (**a**) isabelline wheatear (*Oenanthe isabellina*) [30]; (**b**) red-necked grebe (*Podiceps grisegena*) [32].

4.4. Non-Standard Egg Profiles

Occasionally, we can encounter eggs whose shape does not fit our accepted classification (see Section 1). These include elliptical variations that do not conform to the standard ellipse (Equation (30)), such as the already noted cigar-shaped form or profiles with an excessively wide (or narrow) blunt end, and some others. We called this group 'non-standard egg profiles' and tested the suitability of applying the sinusoidal variations (Equations (12)–(26)) to these eggs. Although we were only able to classify five eggs into this category, the results of the description using all five variations were satisfactory and demonstrated the following:

I. Incomplete polynomial (Equations (12)–(14)), ε = 2.20%.
II. Power function (Equations (15)–(17)), ε = 2.46%.
III. Rational function (Equations (18)–(20)), ε = 2.00%.
IV. The product of x and the exponential function (Equations (21)–(23)), ε = 2.08%.
V. Exponential combination (Equations (24)–(26)), ε = 2.15%.

The visualization of the contours of actual eggs of irregular shape and their corresponding sinusoids containing a rational sub-function (Equation (19)) is presented in Figure 10.

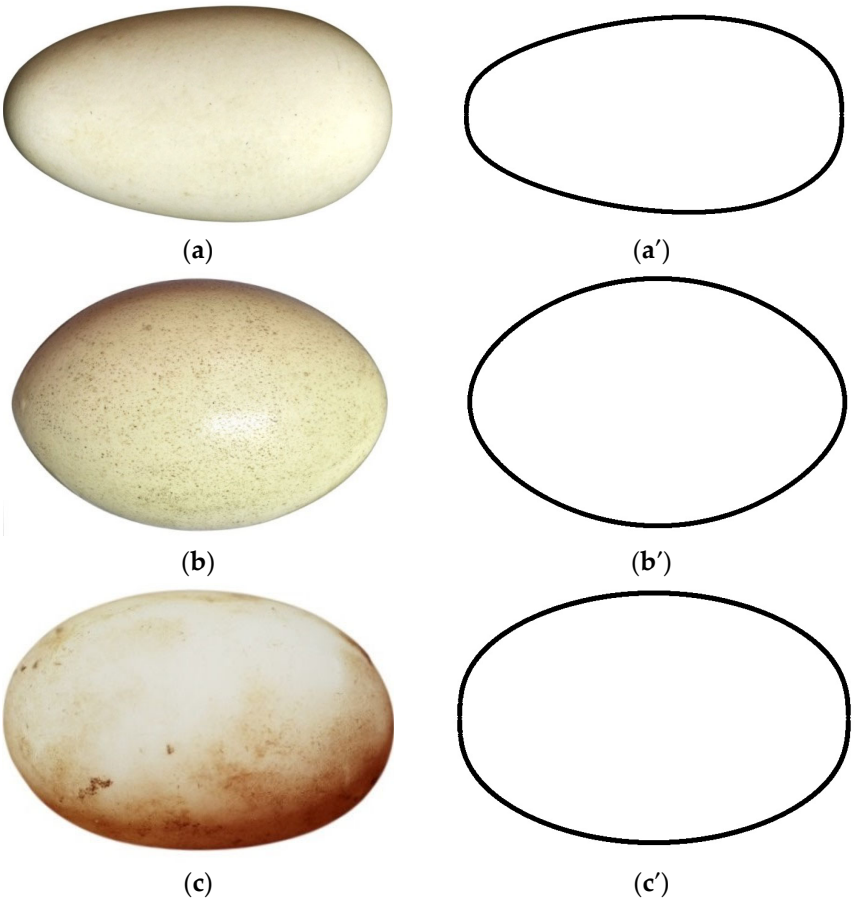

Figure 10. Non-standard shaped eggs (**a**–**c**) in comparison to the 'rational' sine function (Equation (19)) (**a′**–**c′**): (**a**) common swift (*Apus apus*) [96]; (**b**) greater rhea (*Rhea americana*) [97]; (**c**) western pond turtle (*Actinemys marmorata*) [76].

4.5. 'Rational' Sine Function as a New Mathematical Standard of the Ovals

Despite the issue with the biconical eggs, the average ε values across all egg categories were in favor of the 'rational' sine function (Equations (18)–(20)), which demonstrated an accuracy of 2.06%, compared to 2.59% for the incomplete polynomial (Equations (12)–(14)), 2.23% for the power function (Equations (15)–(17)), 2.11% for the product of x and the exponential function (Equations (21)–(23)), and 2.14% for the exponential combination (Equations (24)–(26)).

Despite the somewhat heuristic nature of the final choice, as a result, it was the 'rational' sine function (Equations (18)–(20)) that was finally chosen as the standard mathematical model of the oval, although the difference between the sub-functions was marginal. By and large, all five model variants demonstrated similar, highly accurate results with only minor differences and could be considered standard mathematical relationships for the oval geometric figure. However, we need only one equation that will characterize the oval mathematically, and the choice depends on the accuracy to reproduce the contours of actual eggs of various shapes. Thus, the rational sine wave seemed to be preferable. All the other categories are equally entitled to be considered good models of ovals. Moreover, they can each be used in certain applied tasks. For example, to carry out applied research, e.g., when studying biconical eggs, it might be more appropriate to use a power sine wave. This fact,

however, requires separate, more detailed comparative experiments. Nevertheless, the standard formula for the oval geometric figure will remain the rational sine wave.

To understand what makes it special, and why this particular type of sub-function was preferable, we considered other scientific disciplines where such functions have gained importance. For example, sine functions with a sub-function in the form of an incomplete polynomial (only without considering the degree n) are quite well known in sonar, radar, and laser systems, where they are called 'chirp functions' (e.g., [98,99]).

If we use an even more truncated form of the second-order polynomial (x^2), then the sine of this function will be nothing other than the Fresnel function [100]. This function, or rather the integral of this function, has proven to be key in applied research in optics and quantum mechanics (e.g., [101–103]). Although the sub-function x^2 can be conditionally considered a variant of the power-law dependence bx^c, the sine of such a sub-function has not been used for applied problems. Nevertheless, the power-law dependence itself is an effective mathematical tool for applied problems in biological research. Indeed, this very dependence is what biology terms an *allometric function*, describing how different body parts (or their functions) grow or change at rates that do not scale uniformly with overall body size or with the size of another organ (e.g., [104]). Subsequently, numerous allometric relationships have been obtained in the study of bird eggs [105–109]. Under the conditions of our study, this sub-function (Equation (16)) also demonstrated its effectiveness in the geometric description of biconical eggs.

The exponential function is also very common in biological research, although, like the power function, it has never been used as a sub-function of the sine function. Typically, exponential functions are applicable in biological model processes where growth or decay rates are proportional to the current amount, resulting in J-shaped curves for growth or rapid declines (e.g., [110]). It was precisely due to its widespread use to describe biological and/or other problems [111], as well as its compliance with our initial requirement of $y = 0$ at $x = 0$, that this function was included in the list of variants we used. The exponential combination variant (V), which we examined, has also gained considerable popularity in similar studies. It is often indirectly related to the exponential function (e.g., [112]). Because the exponential combination appears in scientific research as a measure of the relative change, it is quite frequently used in biostatistics (e.g., [113,114]).

In part, because of its widespread use and adequacy in describing both morphological and physiological changes in biological processes, the rational function (variant III) proved to be the best for this study in terms of modeling actual forms. What are the mathematical properties of this function that enable it to demonstrate more adequate results, surpassing the others? Mathematically, a rational function is a ratio of polynomials. In our case, the polynomials have a rather simplified mathematical form, representing incomplete (numerator) and complete (denominator) linear dependencies. Thus, this variant of the rational function represents the simplest case of the so-called Padé approximation—a broad class of rational functions that are used in mathematics and numerical methods as convenient approximating dependencies in many areas (e.g., [115,116]). The versatility of this approximation method has not escaped the attention of biological studies (e.g., [117]) one of which is geometry of egg contours [26]. Consequently, achieving the best match to egg contours using a sine function—with a Padé-based sub-function—is entirely to be expected.

Once we had settled on the oval model, which included a rational sub-function (Equations (18)–(20)), we then investigated its compliance with the mathematical principle characteristic of curvilinear relationships, i.e., the Main Axiom.

4.6. Geometric Correspondence of the Oval Equation to the Main Axiom

Since many mathematical expressions developed to accurately reproduce the geometric contours of eggs proved insufficiently mathematically valid, in that the calculated extremum point did not conform to the coordinate of the B value, we deemed it necessary to perform an appropriate verification of our method. For this purpose, the following derivative Equation (18) was defined:

$$\frac{\partial y}{\partial x} = \frac{B}{2} n \sin^{n-1}\left(\frac{\pi\left(\frac{w}{L}-\frac{1}{2}\right)\frac{x}{L}}{\frac{w}{L}\left(2\frac{x}{L}-1\right)-\frac{1}{2}}\right) \cdot \cos\left(\frac{\pi\left(\frac{w}{L}-\frac{1}{2}\right)\frac{x}{L}}{\frac{w}{L}\left(2\frac{x}{L}-1\right)-\frac{1}{2}}\right) \cdot \frac{\frac{\pi}{L}\left(\frac{w}{L}-\frac{1}{2}\right)\left[\frac{w}{L}\left(2\frac{x}{L}-1\right)-\frac{1}{2}\right]-\pi\left(\frac{w}{L}-\frac{1}{2}\right)\frac{x}{L}\cdot\frac{w}{L}\cdot\frac{2}{L}}{\left[\frac{w}{L}\left(2\frac{x}{L}-1\right)-\frac{1}{2}\right]^2}. \quad (32)$$

The resultant derivative expression (Equation (32)) was equated to 0 after some mathematical transformations:

$$\sin^{n-1}\left(\frac{\pi\left(\frac{w}{L}-\frac{1}{2}\right)\frac{x}{L}}{\frac{w}{L}\left(2\frac{x}{L}-1\right)-\frac{1}{2}}\right) \cdot \cos\left(\frac{\pi\left(\frac{w}{L}-\frac{1}{2}\right)\frac{x}{L}}{\frac{w}{L}\left(2\frac{x}{L}-1\right)-\frac{1}{2}}\right) \cdot \frac{1}{\left[\frac{w}{L}\left(2\frac{x}{L}-1\right)-\frac{1}{2}\right]^2} = 0. \quad (33)$$

The feasibility of Equation (33) can be written as a system of three equations:

$$\begin{cases} \sin^{n-1}\left(\frac{\pi\left(\frac{w}{L}-\frac{1}{2}\right)\frac{x}{L}}{\frac{w}{L}\left(2\frac{x}{L}-1\right)-\frac{1}{2}}\right) = 0 \\ \cos\left(\frac{\pi\left(\frac{w}{L}-\frac{1}{2}\right)\frac{x}{L}}{\frac{w}{L}\left(2\frac{x}{L}-1\right)-\frac{1}{2}}\right) = 0 \\ \frac{1}{\left[\frac{w}{L}\left(2\frac{x}{L}-1\right)-\frac{1}{2}\right]^2} = 0 \end{cases}. \quad (34)$$

For the system of Equation (34), there is a restriction that the denominator of each fraction is not equal to 0. That is, we can write:

$$\frac{w}{L}\left(2\frac{x}{L}-1\right)-\frac{1}{2} \neq 0. \quad (35)$$

Wherefrom

$$\frac{x}{L} \neq \frac{1}{4\frac{w}{L}}+\frac{1}{2}. \quad (36)$$

Previously, we [43,118] demonstrated using measurements of actual eggs that the variation in w/L is limited by the range [0 … 0.16]. Substituting any w/L value from this range into Equation (36) yields values from 2 to infinity. Given that x/L is in the range [0 … 1] (Figure 3), values $x/L > 1$ contradict the condition for correctly displaying the egg profile (Figure 3). Therefore, in our further mathematical calculations, we can operate only with the first two equations of system (34), since the third equation obviously cannot satisfy the condition of equality 0. Then, system (34) can be rewritten as follows:

$$\begin{cases} \frac{\pi\left(\frac{w}{L}-\frac{1}{2}\right)\frac{x}{L}}{\frac{w}{L}\left(2\frac{x}{L}-1\right)-\frac{1}{2}} = 0 \\ \frac{\pi\left(\frac{w}{L}-\frac{1}{2}\right)\frac{x}{L}}{\frac{w}{L}\left(2\frac{x}{L}-1\right)-\frac{1}{2}} = \frac{\pi}{2} \end{cases}. \quad (37)$$

Leaving the second equation of system (37) as the only correct condition, we have:

$$x = \frac{L}{2}+w. \quad (38)$$

It is precisely this condition (Equation (38)) that confirms compliance with the Main Axiom, since the extremum point, i.e., the value $y = B/2$, should correspond to the value $x = L/2 + w$ (Figure 3).

Thus, the equation of an oval with a rational sub-function in the form Equation (18), as well as its mathematical modification (Equation (19)), comply with the mathematical laws for geometric figures.

4.7. Mathematical Elegance

One of the criteria for choosing an optimal equation is its so-called mathematical elegance. Paul Dirac (1902–1984), one of the founders of quantum physics, wrote: *"A theory with mathematical beauty is more likely to be correct than an ugly one that fits some experimental data"* [119]. Of course, the primary goal of an equation is its correctness, accuracy, and precision. Only after these requirements are met does the option of mathematical elegance follow. This issue has been examined in many studies [120–124]. As a result, the term mathematical elegance can be broadly defined to encompass concepts such as cognitive simplicity or the ability to retain a formula entirely in one's head, the presence of geometric or physical meaning for each parameter of an equation, and the ease of processing the expression, meaning a reduction in mental effort required to understand the formula. In other words, elegant formulae are those that are easier for the brain to process.

The resultant equation for the oval (Equation (18)) satisfies these criteria. It is relatively simple without the clutter of complex functions or an abundance of coefficients. It does not contain difficult-to-remember numerical values. The initial basis for this equation is a simple sine wave raised to a power, in which the argument is expressed by a simple relationship: x and a linear function. The sine wave, in general, can be thought of as a unique function, since it is considered to be a link between geometry, analysis and algebra, as clearly demonstrated in Euler's formula (e.g., [125]). Each parameter of the equation is understandable for a specialist, and there are only three such parameters in this formula (B/L, w/L and D_p/B). If each parameter has a clear geometric or physical meaning, the formula can claim to be cognitively understandable.

4.8. There Is No Limit to Elegance

One of the fundamental principles of the elegance of a mathematical expression is its cognitive simplicity. That is, the ability to remember and retain the entire formula in one place. Sometimes, rather than memorizing a single complex formula, it is much more convenient to break it down into several simpler, more understandable components. Given this property of the human brain, we decided to follow this approach, using Equation (3.2) (see Supplementary Data) as the basis for further mathematical transformations. Equation (3.2) can be easily transformed into:

$$y = \pm\frac{B}{2}\sin^n\left(\pi\frac{1+k}{\frac{x}{L}+k}\cdot\frac{x}{L}\right), \tag{39}$$

in which $k = c/L$.

Then from Equation (3.3) (see Supplementary Data):

$$k = -\frac{1}{2}\left[1+\frac{1}{2}\left(\frac{w}{L}\right)^{-1}\right]. \tag{40}$$

Introducing the following condition $y = D_p/2$, $x = L/4$ into Equation (40), we obtain:

$$n = \frac{\ln\left(\frac{D_p}{B}\right)}{\ln\left[\sin\left(\pi\frac{1+k}{1+4k}\right)\right]}. \tag{41}$$

To make the coefficient k (Equation (40)) easier to remember, consider $p = -k$. Then finally, the simple, accurate, geometrically adequate and elegant mathematical model for the oval can be expressed with the following set of formulae:

$$y = \pm\frac{B}{2}\sin^n\left(\frac{\pi(1-p)x}{x-pL}\right), \tag{42}$$

or

$$\frac{y}{L} = \pm\frac{1}{2}\cdot\frac{B}{L}\sin^n\left(\pi\frac{1-p}{\frac{x}{L}-p}\cdot\frac{x}{L}\right), \tag{43}$$

in which

$$p = \frac{1}{2}\left[1+\frac{1}{2}\left(\frac{w}{L}\right)^{-1}\right], \tag{44}$$

$$n = \frac{\ln\left(\frac{D_p}{B}\right)}{\ln\left[\sin\left(\pi\frac{1-p}{1-4p}\right)\right]}. \tag{45}$$

5. Conclusions

We contend that, as a result of these studies, the oval is now a valid geometric figure with its own unique, egg-shaped form and respective "elegant" mathematical description. Its construction requires only four measurements (L, B, w and D_p, Figure 3), which combine to form three indices (parameters). Mathematically, the oval is expressed by the classical equation (Equation (42)), with x values ranging from 0 to L, and y values from $-B/2$ to $B/2$. Using the unit form (Equation (43)), we obtain an image of an oval varying along the horizontal axis from 0 to 1. The coefficients p and n included in both equations are calculated according to the corresponding equations (Equations (44) and (45)).

The equation describing the geometry of the oval may also find application in the school curriculum, along with the classical figures of the circle and the ellipse, especially since attempts to expand the mathematical apparatus of the school curriculum with formulae describing the shape of eggs have already been made (e.g., [126–128]).

Supplementary Materials: The following supporting information can be downloaded at: https://www.mdpi.com/article/10.3390/computation14050101/s1, Supplementary Data: Mathematical Transformation of Equations (7)–(11).

Author Contributions: Conceptualization, V.G.N.; methodology, V.G.N.; software, V.G.N.; validation, V.G.N., M.N.R. and D.K.G.; formal analysis, V.G.N. and S.T.O.; investigation, V.G.N.; data curation, V.G.N.; writing—original draft preparation, V.G.N.; writing—review and editing, V.G.N., S.T.O., M.N.R. and D.K.G.; visualization, V.G.N.; supervision, D.K.G.; project administration, M.N.R. All authors have read and agreed to the published version of the manuscript.

Funding: This research received no external funding.

Data Availability Statement: The original contributions presented in this study are included in the article/Supplementary Material. Further inquiries can be directed to the corresponding author.

Conflicts of Interest: The authors declare no conflicts of interest.

Abbreviations

The following abbreviations are used in this manuscript:

a, b, c, k, n, p	Constant coefficients
B	Oval maximum breadth
D_p	Diameter of the oval at a point $L/4$ from its pointed end
L	Oval length
w	Distance by which the maximum breadth of the oval is shifted from its center, i.e., from the point $x = L/2$
ε	Mean percentage error when comparing the oval model with actual egg profiles

References

1. Plutarch. Moralia, Quaestiones Convivales (Table Talk), Book 8, Question 2, "What is Plato's Meaning, When He Says That God Always Plays the Geometer?". In *Moralia*; Loeb Classical Library 425; Clement, P.A.; Hoffleit, H.B., Translators; Harvard University Press: Cambridge, MA, USA, 1969; Volume XIII.
2. Taub, L. What Plato meant by saying that God is always doing geometry: Responses to the question posed by Plutarch in *Table-Talk* 8.2. In *Studies in Premodern Sciences in Memory of Noel M. Swerdlow*; Archimedes; Rochberg, F., Ed.; Springer: Cham, Switzerland, 2026; Volume 74, pp. 87–104. [CrossRef]
3. Gilbert, C. "The egg reopened" again. *Art Bull.* **1974**, *56*, 252–258. [CrossRef]
4. Herz-Fischler, R. Dürer's paradox or why an ellipse is not egg-shaped. *Math. Mag.* **1990**, *63*, 75–85. [CrossRef]
5. Eberhart, S. On Growth and Form in Nature and Art: The Projective Geometry of Plant Buds and Greek Vases. In *Bridges: Mathematical Connections in Art, Music, and Science, 3rd Annual BRIDGES Conference Proceedings, Winfield, KS, USA, 28–30 July 2000*; Sarhangi, R., Ed.; Bridges Conference: Winfield, KS, USA, 2000; pp. 267–278. Available online: https://archive.bridgesmathart.org/2000/bridges2000-267.pdf (accessed on 23 March 2026).
6. Hodos, T. Eggstraordinary artefacts: Decorated ostrich eggs in the ancient Mediterranean world. *Humanit. Soc. Sci. Commun.* **2020**, *7*, 45. [CrossRef]
7. Grady, K. Why Are Artists and Designers so Obsessed with Eggs? House & Garden, Condé Nast Britain. 2023. Available online: https://www.houseandgarden.co.uk/article/interiors-egg-obsession?utm_source=chatgpt.com (accessed on 23 March 2026).
8. Freiberger, M. Perfect Buildings: The Maths of Modern Architecture. Plus Magazine. 2007. Available online: https://plus.maths.org/content/perfect-buildings-maths-modern-architecture (accessed on 23 March 2026).
9. Petrović, M.; Obradović, M.; Mijailović, R. Suitability analysis of Hugelschaffer's egg curve application in architectural and structures' geometry. *Bul. Institutului Politeh. Din Iasi* **2011**, *57*, 115–122. Available online: https://www.researchgate.net/publication/258113014 (accessed on 23 March 2026).
10. Feleki, A.; Nagy, Z. Challenges in Structural Designing of Egg-shaped Steel Structure. In *Challenges in Design and Construction of an Innovative and Sustainable Built Environment, 19th IABSE Congress, Stockholm, Sweden, 21–23 September 2016*; IABSE Congress: Stockholm, Sweden, 2016; pp. 2243–2250. [CrossRef]
11. Obradović, M.; Martinenko, A. A Method for Adjusting the Shape of Semioval Arches Using Hügelschäffer's Construction. In *Proceedings of the 9th International Scientific Conference on Geometry, Graphics and Design in the Digital Age "Mongeometrija 2023", Novi Sad, Serbia, 7–10 June 2023*; Bajšanski, I., Jovanović, M., Eds.; Faculty of Technical Sciences, University of Novi Sad, Serbian Society for Geometry and Graphics: Novi Sad, Serbia, 2023; pp. 205–215. Available online: https://grafar.grf.bg.ac.rs/handle/123456789/3354 (accessed on 23 March 2026).
12. Archiproducts. *Egg Design: The Design Inspired By the Egg*; Archiproducts.com: Bari, Italy, 2025. Available online: https://www.archiproducts.com/en/focus/egg-design-the-design-inspired-by-the-egg_593638 (accessed on 23 March 2026).
13. Weisstein, E.W. *Oval. Wolfram MathWorld*; Wolfram Research, Inc.: Champaign, IL, USA, 2025. Available online: https://mathworld.wolfram.com/Oval.html (accessed on 23 March 2026).
14. Cambridge Dictionary. *Oval*; Cambridge University Press & Assessment: Cambridge, UK, 2026. Available online: https://dictionary.cambridge.org/us/dictionary/english/oval (accessed on 23 March 2026).
15. Farouki, R.T. The Cartesian ovals. *Math. Intell.* **2022**, *44*, 343–353. [CrossRef]
16. Karataş, M. A multi foci closed curve: Cassini oval, its properties and applications. *Doğuş Univ. Derg.* **2013**, *14*, 231–248. Available online: https://dergipark.org.tr/en/pub/doujournal/article/1043098 (accessed on 23 March 2026). [CrossRef]
17. Dixon, R. *Mathographics*; Dover Publications: New York, NY, USA, 1991.
18. Wikimedia Commons. Pied Kingfisher *Ceryle rudis*, Egg, Coll. Museum Wiesbaden, CC BY-SA 3.0 License. Klaus Rassinger and Gerhard Cammerer, Museum Wiesbaden. 2012. Available online: https://commons.wikimedia.org/wiki/File:Ceryle_rudis_MWNH_1249.JPG (accessed on 23 March 2026).

19. Wikimedia Commons. Blue-Spotted Wood Dove *Turtur afer*, Egg, Coll. Museum Wiesbaden, CC BY-SA 3.0 License. Klaus Rassinger and Gerhard Cammerer, Museum Wiesbaden. 2012. Available online: https://commons.wikimedia.org/wiki/File:Turtur_afer_MWNH_0569.JPG (accessed on 23 March 2026).
20. Wikimedia Commons. Harlequin Duck *Histrionicus histrionicus*, Egg, Coll. Museum Wiesbaden, CC BY-SA 3.0 License. Klaus Rassinger and Gerhard Cammerer, Museum Wiesbaden. 2012. Available online: https://commons.wikimedia.org/wiki/File:Histrionicus_histrionicus_MWNH_1024.JPG (accessed on 23 March 2026).
21. Wikimedia Commons. Common redshank *Tringa totanus*, Egg, Coll. Museum Wiesbaden, CC BY-SA 3.0 License. Klaus Rassinger and Gerhard Cammerer, Museum Wiesbaden. 2012. Available online: https://commons.wikimedia.org/wiki/File:Tringa_totanus_MWNH_0210.JPG (accessed on 23 March 2026).
22. Biggins, J.D.; Thompson, J.E.; Birkhead, T.R. Accurately quantifying the shape of birds' eggs. *Ecol. Evol.* **2018**, *19*, 9728–9738. [CrossRef]
23. Mytiai, I.S.; Matsyura, A.V. Geometrical standards in shapes of avian eggs. *Ukr. J. Ecol.* **2017**, *7*, 264–282. [CrossRef] [PubMed]
24. Mytiai, I.S.; Matsyura, A.V.; Jankowski, K.; Mytiai, Z. Mathematical interpretation of avian egg shapes. *Ecol. Monten.* **2020**, *38*, 67–78. [CrossRef]
25. Nishiyama, Y. The mathematics of egg shape. *Int. J. Pure Appl. Math.* **2012**, *78*, 679–689. Available online: https://www.researchgate.net/publication/259604597 (accessed on 23 March 2026).
26. Narushin, V.G.; Romanov, M.N.; Griffin, D.K. Egg and math: Introducing a universal formula for egg shape. *Ann. N. Y. Acad. Sci.* **2021**, *1505*, 169–177. [CrossRef]
27. Narushin, V.G.; Orszulik, S.T.; Romanov, M.N.; Griffin, D.K. A novel approach to egg and math: Improved geometrical standardization of any avian egg profile. *Ann. N. Y. Acad. Sci.* **2023**, *1529*, 61–71. [CrossRef] [PubMed]
28. Preston, F.W. The shapes of birds' eggs: Mathematical aspects. *Auk* **1968**, *85*, 454–463. [CrossRef] [PubMed]
29. Preston, F.W. Shapes of birds' eggs: Extant North American families. *Auk* **1969**, *86*, 246–264. [CrossRef]
30. Wikimedia Commons. Isabelline Wheatear *Oenanthe isabellina*, Egg, Coll. Museum Wiesbaden, CC BY-SA 3.0 License. Klaus Rassinger and Gerhard Cammerer, Museum Wiesbaden. 2012. Available online: https://commons.wikimedia.org/wiki/File:Oenanthe_isabellina_MWNH_1866.JPG (accessed on 23 March 2026).
31. Wikimedia Commons. Rook *Corvus frugilegus*, Egg, Coll. Museum Wiesbaden, CC BY-SA 3.0 License. Klaus Rassinger and Gerhard Cammerer, Museum Wiesbaden. 2012. Available online: https://commons.wikimedia.org/wiki/File:Corvus_frugilegus_MWNH_1322.JPG (accessed on 23 March 2026).
32. Wikimedia Commons. Red-Necked Grebe *Podiceps grisegena*, Egg, Coll. Museum Wiesbaden, CC BY-SA 3.0 License. Klaus Rassinger and Gerhard Cammerer, Museum Wiesbaden. 2012. Available online: https://commons.wikimedia.org/wiki/File:Podiceps_grisegena_MWNH_0120.JPG (accessed on 23 March 2026).
33. Narushin, V.G.; Romanov, M.N.; Lu, G.; Cugley, J.; Griffin, D.K. Digital imaging assisted geometry of chicken eggs using Hügelschäffer's model. *Biosyst. Eng.* **2020**, *197*, 45–55. [CrossRef]
34. Smart, I.H.M. The method of transformed co-ordinates applied to the deformations produced by the walls of a tubular viscus on a contained body: The avian egg as a model system. *J. Anat.* **1969**, *104*, 507–518. Available online: https://pmc.ncbi.nlm.nih.gov/articles/PMC1231951/ (accessed on 23 March 2026).
35. Preston, F.W. The shapes of birds' eggs. *Auk* **1953**, *70*, 160–182. [CrossRef]
36. Biggins, J.D.; Montgomerie, R.; Thompson, J.E.; Birkhead, T.R. Preston's universal formula for avian egg shape. *Ornithology* **2022**, *139*, ukac028. [CrossRef]
37. Carter, T.C. The hen's egg: A mathematical model with three parameters. *Br. Poult. Sci.* **1968**, *9*, 165–171. [CrossRef]
38. Narushin, V.G. The avian egg: Geometrical description and calculation of parameters. *J. Agric. Eng. Res.* **1997**, *68*, 201–205. [CrossRef]
39. Narushin, V.G. Shape geometry of the avian egg. *J. Agric. Eng. Res.* **2001**, *79*, 441–448. [CrossRef]
40. Baker, D.E. A geometric method for determining shape of bird eggs. *Auk* **2002**, *119*, 1179–1186. [CrossRef]
41. Narushin, V.G.; Volkova, N.A.; Dzhagaev, A.Y.; Griffin, D.K.; Romanov, M.N.; Zinovieva, N.A. Coupling artificial intelligence with proper mathematical algorithms to gain deeper insight into the biology of birds' eggs. *Animals* **2025**, *15*, 292. [CrossRef]
42. Narushin, V.G.; Romanov, M.N.; Griffin, D.K. Pear-shaped eggs evolved to maximize the surface area-to-volume ratio, increase metabolism, and shorten incubation time in birds. *Integr. Zool.* **2025**, *20*, 1098–1109. [CrossRef] [PubMed]
43. Narushin, V.G.; Romanov, M.N.; Avni-Magen, N.; Griffin, D.K. Egg Geometrical Index: Encompassing a wide range of avian egg profiles with potential for novel AI applications in research and industry. *J. Food Compos. Anal.* **2025**, *148*, 108143. [CrossRef]
44. Breger, H. Fermat's analysis of extreme values and tangents. *Stud. Leibnitiana* **2013**, *45*, 20–41. Available online: http://www.jstor.org/stable/43695566 (accessed on 23 March 2026). [CrossRef]
45. Johnson, S.G.B.; Steinerberger, S. Intuitions about mathematical beauty: A case study in the aesthetic experience of ideas. *Cognition* **2019**, *189*, 242–259. [CrossRef]
46. De Rosa, D. Mathematical beauty: On the aesthetic qualities of formal language. *Aisthesis* **2024**, *16*, 121–131. [CrossRef]

47. Jaklič, G. Uniform approximation of a circle by a parametric polynomial curve. *Comput. Aided Geom. Des.* **2016**, *41*, 36–46. [CrossRef]
48. Jaklič, G.; Kozak, J. On parametric polynomial circle approximation. *Numer. Algor.* **2018**, *77*, 433–450. [CrossRef]
49. Narushin, V.G.; Orszulik, S.T.; Romanov, M.N.; Griffin, D.K. The pros and cons of the Preston–Biggins egg shape model: A reconsideration case based on mathematical modeling and simulation. *Nonlinear Sci.* **2025**, *4*, 100038. [CrossRef]
50. Narushin, V.G.; Volkova, N.A.; Dzhagaev, A.Y.; Griffin, D.K.; Romanov, M.N.; Zinovieva, N.A. Smart and smarter: Improving on a classic egg shape model. *Theory Biosci.* **2025**, *144*, 305–318. [CrossRef] [PubMed]
51. Narushin, V.G.; Romanov, M.N.; Griffin, D.K. Eggs from the Baker: Simplifying and improving on an under-appreciated oological model. *Mat. Biol. Bioinform.* **2025**, *20*, 437–447. [CrossRef]
52. Gielis, J. A generic geometric transformation that unifies a wide range of natural and abstract shapes. *Am. J. Bot.* **2003**, *90*, 333–338. [CrossRef]
53. Shi, P.; Gielis, J.; Niklas, K.J. Comparison of a universal (but complex) model for avian egg shape with a simpler model. *Ann. N. Y. Acad. Sci.* **2022**, *1514*, 34–42. [CrossRef] [PubMed]
54. Carter, T.C.; Jones, R.M. The hen's egg: Shell shape and size parameters and their interrelations. *Br. Poult. Sci.* **1970**, *11*, 179–188. [CrossRef]
55. Wang, L.; Griffin, D.K.; Romanov, M.N.; Gielis, J. Comparison of two polar equations in describing the geometries of domestic pigeon (*Columba livia domestica*) eggs. *Poult. Sci.* **2024**, *103*, 104196. [CrossRef]
56. Narushin, V.G. Egg geometry calculation using the measurements of length and breadth. *Poult. Sci.* **2005**, *84*, 482–484. [CrossRef]
57. Narushin, V.G.; Volkova, N.A.; Vetokh, A.N.; Sotnikov, D.A.; Volkova, L.A.; Griffin, D.K.; Romanov, M.N.; Zinovieva, N.A. 'Eggology' and mathematics of a quail egg: An innovative non-destructive technology for evaluating egg parameters in Japanese quail. *Food Bioprod. Process.* **2024**, *146*, 49–57. [CrossRef]
58. Narushin, V.G.; Volkova, N.A.; Vetokh, A.N.; Dzhagaev, A.Y.; Sotnikov, D.A.; Volkova, L.A.; Orszulik, S.T.; Griffin, D.K.; Romanov, M.N.; Zinovieva, N.A. Reimagining Archimedes: An innovative and accurate calculation of volumes and asserting another standard method for defining the surface area of quail and any avian eggs. *Food Bioprod. Process.* **2024**, *147*, 327–334. [CrossRef]
59. Moreira, M.A.R.; Ribeiro, K.M.; Silva, É.; Coelho, M.A.N.; Vieira, J.G.; Azevedo, C.T.T.; Ribeiro, K.D. Morphometry and classification of chicken white eggs using computational vision and artificial neural network techniques. *Rev. Contemp.* **2025**, *5*, e7681. [CrossRef]
60. Kang, H.; Hu, Y.; Kaewunruen, S.; Hu, X.; Zhang, J. Geometric and mechanical analysis of selenium-enriched eggs. *J. Mar. Sci. Eng.* **2025**, *13*, 525. [CrossRef]
61. Zhang, J.; Zhu, B.; Wang, F.; Tang, W.; Wang, W.; Zhang, M. Buckling of prolate egg-shaped domes under hydrostatic external pressure. *Thin-Walled Struct.* **2017**, *119*, 296–303. [CrossRef]
62. Zhang, J.; Wang, M.; Wang, W.; Tang, W.; Zhu, Y. Investigation on egg-shaped pressure hulls. *Mar. Struct.* **2017**, *52*, 50–66. [CrossRef]
63. Zhang, J.; Tan, J.; Tang, W.; Zhao, X.; Zhu, Y. Experimental and numerical collapse properties of externally pressurized egg-shaped shells under local geometrical imperfections. *Int. J. Press. Vessel. Pip.* **2019**, *175*, 103893. [CrossRef]
64. Zhang, J.; Dai, M.; Wang, F.; Tang, W.; Zhao, X. Buckling performance of egg-shaped shells fabricated through free hydroforming. *Int. J. Press. Vessel. Pip.* **2021**, *193*, 104435. [CrossRef]
65. Zhang, J.; Cheng, P.; Wang, F.; Tang, W.; Zhao, X. Hydroforming and buckling of an egg-shaped shell based on a petal-shaped perform. *Ocean Eng.* **2022**, *250*, 111057. [CrossRef]
66. Narushin, V.G.; Romanov, M.N.; Griffin, D.K. Egg-inspired engineering in the design of thin-walled shelled vessels: A theoretical approach for shell strength. *Front. Bioeng. Biotechnol.* **2022**, *10*, 995817. [CrossRef]
67. Hou, J.; Chen, L.; Kong, C.; Guan, J.; Zhao, W.; Zhao, X. Development of laminated egg-shaped tsunami shelter structure made of steel-cushioning-steel. *Int. J. Mech. Eng. Appl.* **2024**, *12*, 118–128. [CrossRef]
68. OpenStax. 6.1: Graphs of the Sine and Cosine Functions. In *Precalculus 1e (OpenStax)*; LibreTexts Mathematics, Department of Education Open Textbook Pilot Project, the UC Davis Office of the Provost, the UC Davis Library, the California State University Affordable Learning Solutions Program, and Merlot: Los Angeles, CA, USA, 2021. Available online: https://math.libretexts.org/Bookshelves/Precalculus/Precalculus_1e_(OpenStax)/06%3A_Periodic_Functions/6.01%3A_Graphs_of_the_Sine_and_Cosine_Functions (accessed on 23 March 2026).
69. Köller, J. Egg Curves and Ovals. More Plane Figures. Mathematische Basteleien. 2000. Available online: http://www.mathematische-basteleien.de/eggcurves.htm (accessed on 23 March 2026).
70. Smith, J.O., III. *Mathematics of the Discrete Fourier Transform (DFT): With Audio Applications*, 2nd ed.; W3K Publishing, BookSurge Publishing: Charleston, SC, USA, 2007. Available online: http://ccrma.stanford.edu/ jos/mdft/ (accessed on 23 March 2026).
71. Bird, J. The circle and its properties. In *Bird's Basic Engineering Mathematics*, 8th ed.; Routledge: London, UK, 2021. [CrossRef]
72. Salem, A.B.H. *Geometry of the Ellipse and the Ellipsoid*; Soukra Raoudha: La Soukra, Tunisia, 2021. Available online: https://www.researchgate.net/publication/353342312 (accessed on 23 March 2026).

73. Gardner, M. The superellipse: A curve that lies between the ellipse and the rectangle. *Sci. Am.* **1965**, *213*, 222–234. Available online: https://www.jstor.org/stable/10.2307/24931123 (accessed on 23 March 2026). [CrossRef]
74. Gridgeman, N.T. Lamé ovals. *Math. Gaz.* **1970**, *54*, 31–37. [CrossRef]
75. Mladenova, C.D.; Mladenov, I.M. Geometry of the ovoids: Reptilian eggs and similar symmetric forms. *Geom. Integr. Quantization* **2023**, *25*, 95–116. [CrossRef]
76. Wikimedia Commons. *Actinemys marmorata* Eggs Found in a Pool of a Permanent Creek. CC BY-SA 2.5 License. Pierre Fidenci: Sonoma County, CA, USA, 2006. Available online: https://commons.wikimedia.org/wiki/File:Clemmys_marmorata03.jpg (accessed on 23 March 2026).
77. Wikimedia Commons. *Apteryx australis*, Egg. CC BY-SA 4.0 License. David J. Stang, Delaware Museum of Natural History. 2008. Available online: https://commons.wikimedia.org/wiki/File:Apteryx_australis_1zz.jpg (accessed on 23 March 2026).
78. Pasini, D. On the biological shape of the Polygonaceae Rheum petiole. *Int. J. Des. Nat. Ecodyn.* **2008**, *3*, 39–64. [CrossRef]
79. Zhang, L.; Niklas, K.J.; Niinemets, Ü.; Li, Q.; Yu, K.; Li, J.; Chen, L.; Shi, P. Stomatal area estimation based on stomatal length and width of four Magnoliaceae species: Even "kidney"-shaped stomata are not elliptical. *Trees* **2023**, *37*, 1333–1342. [CrossRef]
80. Huang, W.; Ma, K.; Tan, J.; Wei, M.; Lu, Y. Superellipse equation describing the geometries of *Abies alba* tree rings. *Plants* **2024**, *13*, 3487. [CrossRef]
81. Wikimedia Commons. Category: Eggs of the Natural History Collections of the Museum Wiesbaden. 2014. Available online: https://commons.wikimedia.org/wiki/Category:Eggs_of_the_Natural_History_Collections_of_the_Museum_Wiesbaden (accessed on 23 March 2026).
82. Wikimedia Commons. Category: Bird Eggs of the Muséum de Toulouse. 2019. Available online: https://commons.wikimedia.org/wiki/Category:Bird_eggs_of_the_Mus%C3%A9um_de_Toulouse (accessed on 23 March 2026).
83. Makridakis, S.; Andersen, A.; Carbone, R.; Fildes, R.; Hibon, M.; Lewandowski, R.; Newton, J.; Parzen, E.; Winkler, R. The accuracy of extrapolation (time series) methods: Results of a forecasting competition. *J. Forecast.* **1982**, *1*, 111–153. [CrossRef]
84. Huttenlocher, D.P.; Klanderman, G.A.; Rucklidge, W. Comparing images using the Hausdorff distance. *IEEE Trans. Pattern Anal. Mach. Intell.* **1993**, *15*, 850–863. [CrossRef]
85. Aydin, O.U.; Taha, A.A.; Hilbert, A.; Khalil, A.A.; Galinovic, I.; Fiebach, J.B.; Frey, D.; Madai, V.I. On the usage of average Hausdorff distance for segmentation performance assessment: Hidden error when used for ranking. *Eur. Radiol. Exp.* **2021**, *5*, 4. [CrossRef] [PubMed]
86. Willmott, C.; Matsuura, K. Advantages of the Mean Absolute Error (MAE) over the Root Mean Square Error (RMSE) in assessing average model performance. *Clim. Res.* **2005**, *30*, 79–82. [CrossRef]
87. Hodson, T.O. Root-mean-square error (RMSE) or mean absolute error (MAE): When to use them or not. *Geosci. Model Dev.* **2022**, *15*, 5481–5487. [CrossRef]
88. Chai, T.; Draxler, R.R. Root mean square error (RMSE) or mean absolute error (MAE)?—Arguments against avoiding RMSE in the literature. *Geosci. Model Dev.* **2014**, *7*, 1247–1250. [CrossRef]
89. Ursinus, O. Kurvenkonstruktionen für den Flugzeugentwurf. *Flugsport* **1944**, *36*, 15–18. Available online: https://scholar.google.com/scholar?hl=en&as_sdt=0%2C5&q="Kurvenkonstruktionen+für+den+Flugzeugentwurf" (accessed on 23 March 2026).
90. Schmidbauer, H. Eine exakte Eierkurvenkonstruktion mit technischen Anwendungen. *Elem. Math.* **1948**, *3*, 67–68. Available online: https://scholar.google.com/scholar?hl=en&q="Eine+exakte+Eierkurvenkonstruktion+mit+technischen+Anwendungen" (accessed on 23 March 2026).
91. Petrović, M.; Obradović, M. The Complement of the Hugelschaffer's Construction of the Egg Curve. In *Proceedings of the 25th National and 2nd International Scientific Conference "Mongeometrija 2010", Belgrade, Serbia, 24–27 June 2010*; Nestorović, M., Ed.; Faculty of Architecture, University of Belgrade, Serbian Society for Geometry and Graphics: Belgrade, Serbia, 2010; pp. 520–531. Available online: https://grafar.grf.bg.ac.rs/handle/123456789/2050 (accessed on 23 March 2026).
92. Obradović, M.; Malesević, B.; Petrović, M.; Đukanović, G. Generating curves of higher order using the generalisation of Hügelschäffer's egg curve construction. *Sci. Bull. Politeh. Univ. Timiş. Trans. Hydrotech.* **2013**, *58*, 110–114. Available online: https://www.researchgate.net/publication/332530776 (accessed on 23 March 2026).
93. Narushin, V.G.; Romanov, M.N.; Griffin, D.K. A novel model for eggs like pears: How to quantify them geometrically with two parameters? *J. Biosci.* **2023**, *48*, 35. [CrossRef] [PubMed]
94. Wikimedia Commons. Thick-Billed Murre *Uria lomvia*, Egg, Coll. Museum Wiesbaden, CC BY-SA 3.0 License. Klaus Rassinger and Gerhard Cammerer, Museum Wiesbaden. 2012. Available online: https://commons.wikimedia.org/wiki/File:Uria_lomvia_MWNH_2182.JPG (accessed on 23 March 2026).
95. Wikimedia Commons. Chukar Partridge *Alectoris chukar*, Egg, Coll. Museum Wiesbaden, CC BY-SA 3.0 License. Klaus Rassinger and Gerhard Cammerer, Museum Wiesbaden. 2012. Available online: https://commons.wikimedia.org/wiki/File:Alectoris_chukar_MWNH_1084.JPG (accessed on 23 March 2026).

96. Wikimedia Commons. Common Swift *Apus apus*, Egg, Coll. Museum Wiesbaden, CC BY-SA 3.0 License. Klaus Rassinger and Gerhard Cammerer, Museum Wiesbaden. 2012. Available online: https://commons.wikimedia.org/wiki/File:Apus_apus_MWNH_1247.JPG (accessed on 23 March 2026).
97. Wikimedia Commons. Greater Rhea Rhea Americana, Egg, Coll. Museum Wiesbaden, CC BY-SA 3.0 License. Klaus Rassinger and Gerhard Cammerer, Museum Wiesbaden. 2012. Available online: https://commons.wikimedia.org/wiki/File:Rhea_americana_MWNH_0003.JPG (accessed on 23 March 2026).
98. Smith, S.W. *Digital Signal Processing. A Practical Guide for Engineers and Scientists*; Newnes, Elsevier Science: Burlington, MA, USA, 2003. Available online: https://books.google.com/books?id=CdtQBAAAQBAJ (accessed on 23 March 2026).
99. Sahay, S.B.; Meghasyam, T.; Roy, R.K.; Pooniwala, G.; Chilamkurthy, S.; Gadre, V. Parameter estimation of linear and quadratic chirps by employing the fractional Fourier transform and a generalized time frequency transform. *Sadhana-Acad. Proc. Eng. Sci.* **2015**, *40*, 1049–1075. [CrossRef]
100. Fresnel, A. *Premier Mémoire sur la Diffraction de la Lumière. Mémoire Adressé à l'Académie des Sciences le 15 Octobre 1815. Le Texte Présenté ici a été Publié Dans les Œuvres Complètes d'Augustin Fresnel*; MM. Henri de Senarmont, Emile Verdet et Léonor Fresnel, Impr. Impériale: Paris, France, 1866–1870. [CrossRef]
101. Abedin, K.M.; Islam, M.R.; Haider, A.F.M.Y. Computer simulation of Fresnel diffraction from rectangular apertures and obstacles using the Fresnel integrals approach. *Opt. Laser Technol.* **2007**, *39*, 237–246. [CrossRef]
102. Zamboni-Rached, M.; Recami, E.; Balma, M. Simple and effective method for the analytic description of important optical beams when truncated by finite apertures. *Appl. Opt.* **2012**, *51*, 3370–3379. [CrossRef]
103. Sandoval-Hernandez, M.; Vazquez-Leal, H.; Hernandez-Martinez, L.; Filobello-Nino, U.A.; Jimenez-Fernandez, V.M.; Herrera-May, A.L.; Castaneda-Sheissa, R.; Ambrosio-Lazaro, R.C.; Diaz-Arango, G. Approximation of Fresnel integrals with applications to diffraction problems. *Math. Probl. Eng.* **2018**, *2018*, 4031793. [CrossRef]
104. Shingleton, A.W. Allometry: The study of biological scaling. *Nat. Sci. Educ.* **2010**, *3*, 2. Available online: https://www.nature.com/scitable/knowledge/library/allometry-the-study-of-biological-scaling-13228439/ (accessed on 23 March 2026).
105. Paganelli, C.V.; Olszowka, A.; Ar, A. The avian egg: Surface area, volume, and density. *Condor* **1974**, *76*, 319–325. [CrossRef]
106. Rahn, H.; Ar, A. The avian egg: Incubation time and water loss. *Condor* **1974**, *76*, 147–152. [CrossRef]
107. Ar, A.; Rahn, H. Interdependence of gas conductance, incubation length, and weight of the avian egg. In *Respiratory Function in Birds, Adult and Embryonic. Proceedings in Life Sciences*; Piiper, J., Ed.; Springer: Berlin/Heidelberg, Germany, 1978; pp. 227–236. [CrossRef]
108. Rahn, H.; Huntington, C.E. Eggs of leach's storm petrel: O_2 Uptake, water loss, and microclimate of the nest. *Comp. Biochem. Physiol. Part A Physiol.* **1988**, *91*, 519–521. [CrossRef]
109. Rahn, H.; Paganelli, C.V. The initial density of avian eggs derived from the tables of Schönwetter. *J. Ornithol.* **1989**, *130*, 207–215. [CrossRef]
110. Souza, R.N.; Mesquita, A.L.; Tavares, H.R. Population growth model and avalanche. *Rev. Fisio Ter.* **2024**, *28*, 132. [CrossRef]
111. Budinski, N. Exponential functions through a real-world context. *Open Sch. J. Open Sci.* **2020**, *3*, 24891. [CrossRef]
112. Zwietering, M.H.; Jongenburger, I.; Rombouts, F.M.; Van't Riet, K.J.A.E.M. Modeling of the bacterial growth curve. *Appl. Environ. Microbiol.* **1990**, *56*, 1875–1881. [CrossRef]
113. Sperandei, S. Understanding logistic regression analysis. *Biochem. Med.* **2014**, *24*, 12–18. [CrossRef]
114. Clement, L. 6. Simple Linear Regression. In *PSLS20: Practical Statistics for the Life Sciences, Gulbenkian Training Programme in Bioinformatics (GTPB) Courses*; Instituto Gulbenkian de Ciência: Oeiras, Portugal, 2020. Available online: https://gtpb.github.io/PSLS20/pages/06-linearRegression/06-linearRegression.html (accessed on 23 March 2026).
115. Apresyan, L.A. Pade approximants (review). *Radiophys. Quantum Electron.* **1979**, *22*, 449–466. [CrossRef]
116. Baker, G.A., Jr.; Graves-Morris, P. *Padé Approximants*, 2nd ed.; Cambridge University Press: New York, NY, USA, 1996. [CrossRef]
117. Kalospyros, S.A.; Nikitaki, Z.; Kyriakou, I.; Kokkoris, M.; Emfietzoglou, D.; Georgakilas, A.G. A mathematical radiobiological model (MRM) to predict complex DNA damage and cell survival for ionizing particle radiations of varying quality. *Molecules* **2021**, *26*, 840. [CrossRef] [PubMed]
118. Narushin, V.G.; Romanov, M.N.; Salamon, A.; Kent, J.P.; Griffin, D.K. Creating a simulated virtual collection of avian egg shapes. In *Handbook of Egg Sensing Technology*; Khaliduzzaman, A., Ahad, M.A.R., Kamruzzaman, M., Aboonajmi, M., Eds.; (in print). CRC Press: Boca Raton, FL, USA, 2026. Available online: https://books.google.com/books?id=a4fc0QEACAAJ (accessed on 23 March 2026).
119. Bokulich, A. *Reexamining the Quantum–Classical Relation. Beyond Reductionism and Pluralism*; Cambridge University Press: Cambridge, UK, 2008. Available online: https://bokulich.org/wp-content/uploads/2020/06/reexamin-q-c-book_bokulich.pdf (accessed on 23 March 2026).
120. Reber, R.; Schwarz, N.; Winkielman, P. Processing fluency and aesthetic pleasure: Is beauty in the perceiver's processing experience? *Pers. Soc. Psychol. Rev.* **2004**, *8*, 364–382. [CrossRef]

121. Breitenbach, A. V—Aesthetics in science: A Kantian proposal. *Proc. Aristot. Soc.* **2013**, *113*, 83–100. [CrossRef]
122. Zeki, S.; Romaya, J.P.; Benincasa, D.M.; Atiyah, M.F. The experience of mathematical beauty and its neural correlates. *Front. Hum. Neurosci.* **2014**, *8*, 68. [CrossRef] [PubMed]
123. Cellucci, C. Mathematical beauty, understanding, and discovery. *Found. Sci.* **2015**, *20*, 339–355. [CrossRef]
124. Schwarz, N.; Jalbert, M.; Noah, T.; Zhang, L. Metacognitive experiences as information: Processing fluency in consumer judgment and decision making. *Consum. Psychol. Rev.* **2021**, *4*, 4–25. [CrossRef]
125. Moskowitz, M.A. *A Course in Complex Analysis in One Variable*; World Scientific: Singapore, 2002. [CrossRef]
126. Maasz, J.; Siller, H.S. Mathematics and eggs. In *Real-World Problems for Secondary School Mathematics Students*; Maasz, J., O'Donoghue, J., Eds.; Sense Publishers: Rotterdam, The Netherlands, 2011; pp. 239–256. [CrossRef]
127. Siller, H.-S. Mathematics and eggs—Do those two terms have something in common? *Simul. Notes Eur.* **2011**, *21*, 61–66. Available online: https://www.sne-journal.org/fileadmin/user_upload_sne/SNE_Issues_OA/SNE_21_2/articles/sne.21.2.10055.en.OA.pdf (accessed on 23 March 2026). [CrossRef]
128. Narushin, V.G.; Romanov, M.N.; Griffin, D.K. What comes first: The egg or the mathematics? Review article. *Biol. Bull.* **2023**, *50*, 237–243. [CrossRef]